# Frequency-dependent attenuation-compensation functions for ultrasonic signals backscattered from random media

Michael L. Oelze[a] and William D. O'Brien, Jr.
*Bioacoustics Research Laboratory, Department of Electrical and Computer Engineering, University of Illinois, 405 North Mathews, Urbana, Illinois 61801*

(Received 18 July 2001; accepted for publication 24 December 2001)

Estimations of scattering parameters, such as average scatterer diameter, from rf signals backscattered from random media (tissues) are made from the frequency dependence of the rf signal. The frequency dependence of the rf signal backscattered from the medium is seen in the normalized power spectrum. The normalized power spectrum is found by taking the squared magnitude of the Fourier transform of the rf signal gated over a region of interest and dividing by some reference spectrum. If the medium has a frequency-dependent attenuation then the shape of the normalized power spectrum will be affected by the frequency-dependent attenuation and the time duration of the gated signal. Not accounting for the frequency-dependent attenuation leads to poor estimations of scatterer parameters. Larger attenuation and longer time gates give poorer estimates of scatterer parameters without attenuation compensation. Several attenuation-compensation functions have been used to account for the attenuation losses to the normalized power spectrum. A new attenuation-compensation function is proposed and compared with the other attenuation-compensation routines. The new attenuation-compensation function is shown to give improved estimates over previous attenuation-compensation functions for scatterers that follow a Gaussian form factor. © *2002 Acoustical Society of America.*
[DOI: 10.1121/1.1452743]

PACS numbers: 43.80.Vj, 43.80.Qf [FD]

## I. INTRODUCTION

Clinical ultrasound B-mode images of tissues aid in diagnosis of disease. B-mode images are constructed from envelop-detected backscattered echoes that may contain information about the structure of the biological media. The frequency spectra of rf backscattered echos have been used to noninvasively investigate and parametrize small structures in tissues.[1–9] Information about the structures can be obtained by relating the frequency dependence of the measured spectrum to theoretical predictions.

In many cases the medium (tissues) can be approximated as a random distribution of small scatterers or particles. The frequency spectrum of signals scattered from these particles depends on their average size, shape, distribution, and acoustic impedance. Models have been developed to predict the interaction of sound with a random distribution of scatterers.[10,11] Commonly, tissue scattering theory is described by spatial correlation function models.

The spatial correlation function models assume weak scattering theory, i.e., the incident wave is scattered only once and multiple scattering from particles is assumed to be negligible. A theoretical scattered power spectrum is related to the spatial correlation function through an acoustic intensity form factor.[7] The form factor is determined by evaluating the Fourier transform of the correlation function for the tissue medium. The form (or shape) factor gives the frequency dependence of the normalized power spectrum from the scattering in terms of the assumed shape and distribution of the scatterers.

The frequency dependence of the normalized power spectrum measured from the backscattered echoes can be related to the form factor. The average effective scatterer size and concentration of scatterers can be estimated from the relation between the normalized power spectrum and the modeled form factor. If the attenuation is not negligible and if the attenuation has a frequency dependence, which is almost always the case, then a compensation function is needed to account for the frequency-dependent losses to the normalized power spectrum. As longer gated segments are used to obtain the normalized power spectrum, the effects of frequency-dependent attenuation increases. Assuming that scattering is homogeneous over the length of the gated segment (stationary), then on average the difference between wavelets scattered near the beginning of the time gate and those scattered near the end will be the frequency-dependent losses. If the effects of frequency-dependent attenuation are not properly taken into account, estimations of scatterer properties from the normalized power spectrum will be incorrect.

This work examines the effects of using different attenuation-compensation functions to account for losses to the normalized power spectrum taken from gated signals. Frequency-dependent attenuation losses come from propagation between the gated region and the source (intervening medium) and over the length of the gated region itself. The accuracy of scatterer estimates depends on the compensation of both propagation regions. This paper focuses on the compensation of attenuation losses to backscattered signals over

[a]Electronic mail: oelze@brl.uiuc.edu

the gated length. A new attenuation-compensation function is proposed and compared with existing attenuation-compensation functions to determine the best compensation function to use in a particular attenuating media. Section II outlines the theory describing the development of a new attenuation-compensation function. Section III compares the new attenuation-compensation function with other attenuation-compensation functions. Section IV examines the attenuation-compensation functions for large attenuation or long gate length. Section V gives some concluding remarks about the compensation of backscattered signals.

## II. ATTENUATION-COMPENSATION TECHNIQUES

### A. Derivation of attenuation-compensation functions

Scatterer properties of random scattering media are estimated from the frequency dependence of the normalized power spectrum through the form factor. One form factor that has been shown to model the scattering from many soft tissues well is the Gaussian form factor[2,4–8,12]

$$F_{\text{Gauss}}(2k) = e^{-0.827k^2 a_{\text{eff}}^2}, \tag{1}$$

where $k$ is the acoustic wave number, and $a_{\text{eff}}$ is the average effective radius of the scatterers. The Gaussian form factor describes spherical scattering sources with impedance that varies continuously from the surrounding tissue. The average scatterer size can be estimated from measurements of the form factor.

The form factor is defined as the ratio of the backscatter coefficient, $\sigma_b$, for the scattering medium to the backscatter coefficient of a medium consisting of point scatterers,[6]

$$F(2k) = \frac{\sigma_b}{\sigma_0}, \tag{2}$$

where $\sigma_0$ is backscatter coefficient for point scatterers. Equation (2) gives a theoretical description of the scattering that can be related to actual acoustic measurements through the normalized power spectrum. The normalized power spectrum is related to the form factor through the backscatter coefficient[6]

$$\sigma_b = \frac{CR^2}{A_0 L} W_{\text{meas}}(f), \tag{3}$$

where $C$ is a constant used to normalize the effects of a gating function on the backscattered echo and the effects of the beam of the transducer, $A_0$ is the area of the transducer face, $L$ is the length of the gated segment, $R$ is the on-axis distance between the transducer and the proximal surface of the gated region, and $W_{\text{meas}}(f)$ is the normalized power spectrum. Typically, the normalized power spectrum is measured from a region of interest (ROI) and is an average of the spectral contributions from rf time signals within the specified region. The measured power spectrum from a single rf line in the ROI is the magnitude squared of the Fourier transform, FT($f$), of the backscattered time signal gated according to the length, $L$, of the ROI. The normalized power spectrum is given by averaging each measured power spectrum in the ROI and dividing by a reference spectrum[7,13]

$$W_{\text{meas}}(f) = \frac{A(f,L)}{N} \sum_{m=1}^{N} \frac{|\text{FT}_m(f)|^2}{|\text{FT}_{\text{ref}}(f)|^2} = A(f,L) W_{\text{atten}}(f), \tag{4}$$

where $N$ is the number of gated segments to be averaged and $A$ is an attenuation-compensation function. The reference spectrum takes out the effects of the equipment on the measurement and is found by the substitution technique.[1,14] The attenuation-compensation function is unitless and depends on the frequency-dependent attenuation coefficient (Np/cm) in the gated length, the length of the gated signal, and the propagation losses in the intervening medium. The frequency dependence of the normalized power spectrum is used to make estimates of average scatterer size.

Accounting for the effects of frequency-dependent attenuation is necessary to accurately estimate scatterer properties such as the average scatterer diameter and concentration. Point attenuation compensation has been used in the past to compensate for signal loss when the gated segment is short or the attenuation is small.[6,7] The normalized power spectrum is compensated for round-trip attenuation losses using point compensation by

$$W_{\text{meas}}(f) = W_{\text{atten}}(f) e^{4\alpha_0(f)x_0} e^{4\alpha(f)L/2}, \tag{5}$$

where $x_0$ is the distance between the source and the gated region, $L/2$ is the distance from the edge of the gated region to the middle of the gated region, and $\alpha_0(f)$, $\alpha(f)$ are the frequency-dependent attenuation coefficients in Np/cm for the intervening medium and over the gated region, respectively. The attenuation over the gated region is assumed to be constant.

The simulations in Sec. III will show that when longer gated segments are used or the medium has higher attenuation, i.e., $\alpha(f)L > 0.5$, point compensation does not correctly account for the frequency-dependent effects of attenuation on the normalized power spectrum. The justification for using longer gate lengths is that better estimates of scatterer properties can be obtained.[15] Chen *et al.* compared experimental measurements of backscatter coefficients (power spectrum) from phantoms of glass beads in agar using gate lengths of 3 mm, 7.7 mm, and 3 cm with theoretical predictions.[15] The results of the experiments by Chen *et al.* showed that the longer gate lengths followed more closely the theoretical spectrum over the largest frequency range. When $\alpha(f)L > 0.5$, point attenuation compensation tends to overcompensate for the frequency dependence of the normalized power spectrum. Overcompensating for the frequency-dependent losses causes the underestimation of average scatterer diameters. Figure 1 shows how the overcompensation of frequency-dependent attenuation leads to underestimation of scatterer sizes. From Fig. 1 it is seen that the form factor for smaller scatterers has a flatter slope than for larger scatterers. Typically, attenuation increases with increasing frequency. If an attenuation-compensation function overcompensates, then the large frequencies will be overcompensated more than the lower frequencies. The net effect is to raise the overall slope of the measured form factor causing an underestimation of the scatterer size.

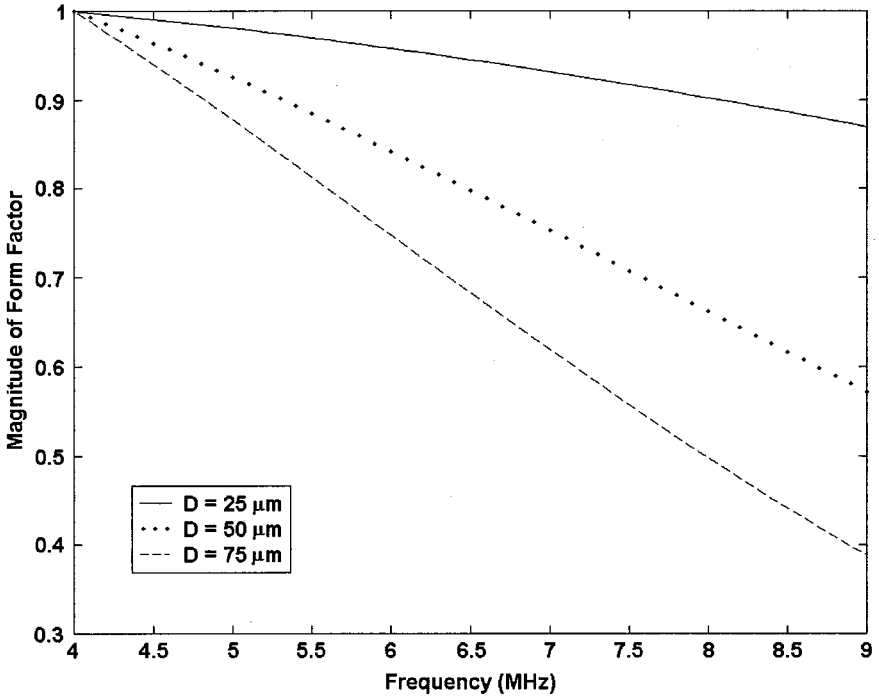


FIG. 1. The relative magnitude of the Gaussian form factor over the frequency range of 4–9 MHz for scatterers with diameters of 25, 50, and 75 $\mu$m.

In order to obtain more accurate estimates of scatterer diameters, the effects of larger attenuation or attenuation from longer gated signals need to be more accurately compensated. An approximate closed form attenuation-compensation function, $A$, for backscattered returns was first introduced by Sigelmann and Reid[14] and utilized by O'Donnell and Miller.[16] The O'Donnell and Miller attenuation-compensation term is given by

$$W_{\text{meas}}(f)=W_{\text{atten}}(f)A_{\text{OM}}(f,L),$$

where

$$A_{\text{OM}}(f,L)=e^{4\alpha_0(f)x_0}\left[\frac{4\alpha(f)L}{1-e^{-4\alpha(f)L}}\right]. \tag{6}$$

The term in square brackets accounts for the frequency-dependent attenuation losses over the gated region. The term outside the square brackets accounts for the round-trip frequency-dependent attenuation losses between the gated region and the source. The O'Donnell and Miller compensation function is based on the approximation of small attenuation or short gate length over the frequencies of interest.[16] The simulations of Sec. III will show that the compensation term used by O'Donnell and Miller gives better estimations for scatterer estimations than the point attenuation-compensation term at longer gate lengths and larger attenuations. However, as $\alpha(f)L$ becomes larger the O'Donnell and Miller compensation function begins to yield increasingly inaccurate estimates of scatterer diameters.

To improve scatterer estimations, an alternative attenuation-compensation function is proposed. Consider a signal of the form, $g_L(t)$, representing a rf time sequence from a gated length, $L$, in a scattering medium. The function, $g_L(t)$, is the convolution of an impulse response, $p(t)$ (incorporating the electromechanical characteristics of the transducer and diffraction), and a scattering function, $r_L(t)$, from randomly spaced, identical particles,[17,18]

$$g_L(t)=p(t)*r_L(t). \tag{7}$$

The Fourier transform of the signal is given by

$$G_L(f)=P(f)R_L(f). \tag{8}$$

The Fourier spectrum, $R_L(f)$, over the rectangular gated length, $L$, is defined as

$$R_L(f)=\int_0^{2L/c} r_L(t)e^{-i2\pi ft}\,dt \tag{9}$$

and can be broken into $N$ discrete integrals of length $dx$,

$$\begin{aligned}R_L(f)=&\int_0^{2\,dx/c} r_L(t)e^{-i2\pi ft}\,dt\\&+\int_{2\,dx/c}^{2(2)dx/c} r_L(t)e^{-i2\pi ft}dt+\cdots\\&+\int_{2(N-1)dx/c}^{2N\,dx/c} r_L(t)e^{-i2\pi ft}\,dt.\end{aligned}$$

Letting $r_{dx}(t)$ represent the scattering function of randomly spaced identical scatterers from some small $dx$ segment then

$$\begin{aligned}r_{dx}(t)=&s(t+t_0)+s(t+t_0+2d_2/c)\\&+s(t+t_0+2d_3/c)+\cdots,\end{aligned} \tag{10}$$

where $c$ is the speed of sound in the medium and $d_i$ represents the individual scatterer spacings. The Fourier transform of $r_{dx}(t)$ is then given by

$$\begin{aligned}R_{dx}(f)=&S(f)\\&\times[1+e^{i2\pi f(2d_1/c)}+e^{i2\pi f(2d_2/c)}+\cdots]e^{-i2\pi t_0},\\R_{dx}(f)=&S(f)[1+\Phi(f,x)]e^{i2\pi ft_0},\end{aligned} \tag{11}$$

where $\Phi(f,x)$ is a random phase caused by the interference between the scattering from particles in the $dx$ section located at a position, $x$. Essentially, $\Phi(f,x)$ sums together all of the random phase contributions of the identical particles caused by their random spacings. For a small number of particles it is expected that $\Phi(f,x)\neq 0$ but as the number of particles, $N_p$, becomes large, $\Phi(f,x)\rightarrow 0$. For a particular number density of scatterers within a certain volume then as the volume increases, $N_p$ also increases and $\Phi(f,x)\rightarrow 0$.

Assuming that consecutive $dx$ sections are small and are homogeneous with scattering (similar number density of scatterers and scatterer type) then the round-trip propagation loss can be incorporated in Eq. (11) by

$$R_{dx}(f)\approx S(f)[1+\Phi(f,x)]e^{i2\pi ft_0}e^{-2\alpha(f)x}, \tag{12}$$

where $\alpha(f)$ is the frequency-dependent attenuation in the gated region (assumed constant). The spatial average Fourier spectrum of the scattering function from the length, $L$, is the sum of all the $dx$ segments in the total length divided by $L$,

$$R_L(f)=S(f)e^{-i2\pi ft_0}\frac{1}{L}\int_0^L[1+\Phi(f,x)]e^{-2\alpha(f)x}dx. \tag{13}$$

The second integral term involving $\Phi(f,x)$ is a summation of the random phase points of the identical scatterers in the gated segment, $L$, weighted by the attenuation of the signal at the depth, $x$. The attenuation diminishes the contribution of scatterers from greater propagation distances in the gated length. The attenuation effectively reduces the number of scatterers contributing to the phase summation. If the effective number of scatterers in the segment, $L$, is large then the integral term involving $\Phi(f,x)$ will be negligible. Integration of the first term yields

$$R_L(f)=S(f)e^{i2\pi ft_0}\frac{1-e^{-2\alpha(f)L}}{2\alpha(f)L}. \tag{14}$$

The power spectrum for the gated segment of length, $L$, is defined as

$$W_{\text{meas}}(f)=|G_L(f)|^2e^{-4\alpha_0(f)x_0}, \tag{15}$$

where the exponential term accounts for the round-trip propagation loss of the signal in the intervening medium. Substituting Eqs. (8) and (14) into Eq. (15) gives

$$W_{\text{meas}}(f)=|P(f)|^2|S(f)|^2\frac{(1-e^{-2\alpha(f)L})^2}{4\alpha^2(f)L^2}e^{-4\alpha_0(f)x_0}=\frac{|P(f)|^2|S(f)|^2}{A_{\text{OO}}(\alpha,L)}, \tag{16}$$

where $A_{\text{OO}}(\alpha,L)$ is an attenuation-compensation function (Oelze and O'Brien compensation) for signals gated from a scattering medium.

The O'Donnell and Miller compensation function can be derived by further examination of Eq. (11). The power spectrum of $R_{dx}(f)$ for some small section, $dx$, is given by

$$|R_{dx}(f)|^2=|S(f)|^2|[1+\Phi(f,x)]|^2. \tag{17}$$

Incorporating the round-trip propagation loss yields

$$|R_{dx}(f)|^2\approx|S(f)|^2|[1+\Phi(f,x)]|^2e^{-4\alpha(f)x} \tag{18}$$

for a particular $dx$ segment. The spatial average of the scattered power spectrum from some length, $L$, is the average of the spectra of each $dx$ segment giving

$$|R_L(f)|^2=\frac{|S(f)|^2}{L}\int_0^L|[1+\Phi(f,x)]|^2e^{-4\alpha(f)x}dx. \tag{19}$$

Expanding the terms yields

$$|R_L(f)|^2=\frac{|S(f)|^2}{L}\int_0^L(1+[\Phi+\Phi^*]+\Phi^*\Phi)e^{-4\alpha(f)x}dx. \tag{20}$$

The second and third terms can be considered negligible if a large effective number of scatterers exist in $L$. The normalized power spectrum from the gated length, $L$, will then be given by Eq. (15),

$$W_{\text{meas}}(f)=|P(f)|^2|S(f)|^2\frac{1-e^{-4\alpha(f)L}}{4\alpha(f)L}e^{-4\alpha_0(f)x_0}=\frac{|P(f)|^2|S(f)|^2}{A_{\text{OM}}(\alpha,L)}. \tag{21}$$

Two limiting cases of the attenuation-compensation term are when the quantity $\alpha(f)L$ is small. In the case of small $\alpha(f)L$, keeping only first-order terms in the exponential terms of $A_{\text{OO}}$ and $A_{\text{OM}}$ gives

$$1-e^{-2\alpha(f)L}\approx 2\alpha(f)L$$

and

$$1-e^{-4\alpha(f)L}\approx 4\alpha(f)L,$$

which reduces $A_{\text{OO}}$ and $A_{\text{OM}}$ to

$$A_{\text{OO}}(f,L)=A_{\text{OM}}(f,L)\approx e^{4\alpha_0(f)x_0} \tag{22}$$

or the point attenuation-compensation term. Keeping only the second-order terms yields

$$A_{\text{OO}}(f,L)=A_{\text{OM}}(f,L)\approx e^{4\alpha_0(f)x_0}\left[\frac{1}{1-2\alpha(f)L}\right]. \tag{23}$$

To second order the Oelze and O'Brien attenuation-compensation function and the O'Donnell and Miller function agree.

### B. Error analysis

The difference between the Oelze and O'Brien attenuation-compensation function and the O'Donnell and Miller attenuation-compensation function can be seen by examination of the random phase summation terms that were approximated to be negligible. Neglecting the intervening medium compensation term and looking at the average power spectrum from Eq. (15) including the phase summation terms shows

$$W_{\text{OO}}(f)=\frac{|P(f)|^2|S(f)|^2}{L^2}\times\left|\int_0^L[1+\Phi(f,x)]e^{-2\alpha(f)x}dx\right|^2, \tag{24}$$

$$W_{\mathrm{OO}}(f)=\frac{|P(f)|^2|S(f)|^2}{L^2}\times\left(\frac{1}{A_{\mathrm{OO}}}+\frac{L}{A_{\mathrm{OO}}^{1/2}}\int_0^L(\Phi+\Phi^*)e^{-2\alpha(f)x}dx+\left|\int_0^L\Phi e^{-2\alpha(f)x}dx\right|^2\right)$$

The "error" terms of the Oelze and O'Brien attenuation-compensation function are given by the second and third terms of Eq. (24),

$$\epsilon_{\mathrm{OO}}(f)=\frac{|P(f)|^2|S(f)|^2}{L}\left(\frac{1}{A_{\mathrm{OO}}^{1/2}}\int_0^L(\Phi+\Phi^*)e^{-2\alpha(f)x}dx+\frac{1}{L}\left|\int_0^L\Phi e^{-2\alpha(f)x}dx\right|^2\right). \quad (25)$$

If $\alpha$ is large then $A_{\mathrm{OO}}\rightarrow 4\alpha^2L^2$, giving

$$\epsilon_{\mathrm{OO}}(f)=\frac{|P(f)|^2|S(f)|^2}{L}\left(\frac{1}{2\alpha L}\int_0^L(\Phi+\Phi^*)e^{-2\alpha(f)x}dx+\frac{1}{L}\left|\int_0^L\Phi e^{-2\alpha(f)x}dx\right|^2\right). \quad (26)$$

For the O'Donnell and Miller attenuation-compensation function the error terms can be seen from Eq. (20),

$$\epsilon_{\mathrm{OM}}(f)=\frac{|P(f)|^2|S(f)|^2}{L}\left(\int_0^L(\Phi+\Phi^*)e^{-4\alpha(f)x}dx+\int_0^L|\Phi|^2e^{-4\alpha(f)x}dx\right). \quad (27)$$

One would expect $\Phi(f,x)\rightarrow 0$ for a large number of scatterers. For a small number of random scatterers $\Phi(f,x)$ could not be assumed zero. The larger the gated segment the more likely $\Phi(f,x)\rightarrow 0$.

The trade-off between smaller gate size and better scatterer resolution can be seen from the error terms. The estimates of scatterer sizes are obtained from the term $|S(f)|^2$. Knowing the impulse response, $|P(f)|^2$, and the attenuation-compensation functions, the approximate term, $|S(f)|^2$, can be found from Eq. (16) or (21) by assuming that terms involving $\Phi(f,x)$ are small. However, if a small gate length means few random scatterers, the effects of attenuation may be negligible but the effects of the random scattering spacings on the measured power spectrum will be larger because $\Phi(f,x)\neq 0$. If a large gate length means many random scatterers, the greater the attenuation effect but the greater the likelihood that $\Phi(f,x)\rightarrow 0$. On the other hand, if the attenuation is large such that the effective number of scatterers is reduced to a few, the longer gate length will be of no advantage. What attenuation does is to weight the contribution of the phase points from scatterers at greater depth less than scatterers located at a shallower propagation depth. Attenuation effectively reduces the number of scatterer particles contributing to $\Phi(f,x)$. The effective reduction in scatterer number means it is less likely that $\Phi(f,x)$ will have negligible contribution to the power spectrum from a signal gated from length, $L$. Hence, estimation of scatterer sizes will be more accurate when the attenuation is small as opposed to large.

Comparing the error terms for the Oelze and O'Brien development [Eq. (26)] and the O'Donnell and Miller compensation function [Eq. (27)] shows that for large attenuation the first error term of the Oelze and O'Brien compensation is less than the first error term of the O'Donnell and Miller compensation function. The first terms are identical except for the $1/[2\alpha L]$ factor in the Oelze and O'Brien error term and the factor of 1/2 in the power of the exponent. The $1/[2\alpha L]$ factor and the reduced power in the attenuation exponent of the Oelze and O'Brien error term means that for large attenuation, $\alpha(f)L>1$, the first term of the Oelze and O'Brien term is much less than the O'Donnell and Miller error term. Comparisons of the second error terms also show that the Oelze and O'Brien error is less. Integrating $|\Phi|^2$ over the gate length means that all the summation of the phase points must be greater than or equal to zero. Thus, even without the attenuation and with a large number of scatterers the second term of the error term, Eq. (27), will not sum to zero. Comparisons of the error terms show that the Oelze and O'Brien attenuation-compensation function is superior to the O'Donnell and Miller attenuation-compensation function.

Since the second integral term in Eq. (27) is always positive, the O'Donnell and Miller term will undercompensate the attenuated, gated signal. For a larger gate length, i.e., more scatterers, the second error term of the O'Donnell and Miller attenuation-compensation function increasingly undercompensates the attenuated, gated signal. If the attenuation is larger, then the effective number of scatterers contributing to the undercompensation is less. Thus, the contribution of the second error term in the O'Donnell and Miller attenuation-compensation function is lessened with larger attenuation but increased with longer gate length. In either case, the second term means the O'Donnell and Miller attenuation-compensation function will undercompensate the attenuation losses in a gated signal from random scatterers.

Figure 2 shows the magnitude of three different compensation functions with increasing $\alpha(f)L$. Increasing $\alpha(f)L$ may result from increasing the rectangular gate length or from increasing the attenuation with frequency. Figure 2 shows that the point attenuation-compensation function gives the greatest overall compensation. The O'Donnell and Miller compensation term gives the smallest overall compensation to the attenuation losses. The Oelze and O'Brien compensation term gives an adjustment to the attenuation losses that lies between the point compensation and the O'Donnell and Miller compensation term. As seen in Fig. 2, both the O'Donnell and Miller compensation term and the Oelze and O'Brien compensation term reduce to the point compensation term for small $\alpha(f)L$.

### C. Effects of windowing

The derivations of the attenuation-compensation functions assumed a rectangular window function was applied to the gated time signal. In many applications commercial win-

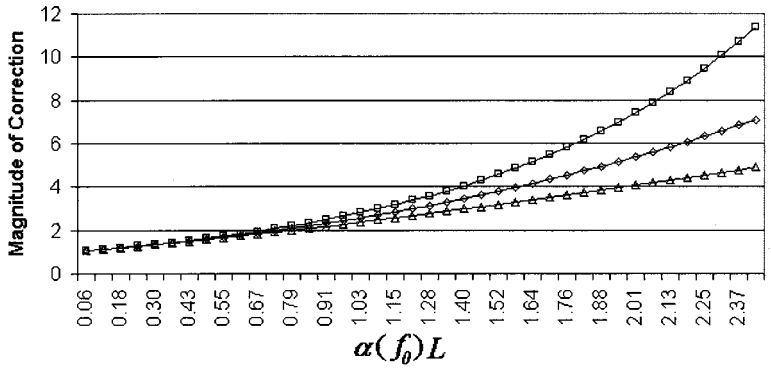


FIG. 2. Comparison of the magnitude of the correction to the normalized power spectrum using three different attenuation-compensation routines; (□) point compensation; (△) O'Donnell and Miller compensation; (◇) Oelze and O'Brien compensation.

dow functions other than the rectangular window are used to gate rf time signals. A window function applied to the time sequence, $g_L(t)$, can be represented by

$$g_L'(t)=h_L(t)g_L(t)=h_L(t)[p(t)*r_L(t)], \tag{28}$$

where $h_L(t)$ is the windowing function. The Fourier transform of the sequence $g_L'(t)$ is given as

$$G_L'(f)=H(f)*[P(f)R(f)], \tag{29}$$

where the Fourier spectrum of the window function is convolved with the impulse spectrum and the scattered signal spectrum. The convolution with the scattered spectrum means that the window function spectrum will also be convolved with the attenuation-compensation function derived using a rectangular window.

To obtain the attenuation-compensation function for any arbitrary window function it is necessary to deconvolve the window spectrum from the attenuation-compensation function derived using a rectangular window. The deconvolution is carried out by examining some small segment, *dx*, of the windowed signal, $g_L'(t)$. For a small *dx* segment the window function varies slowly compared to the scattered signal. The window function can then be approximated as a rectangular window with amplitude, $h(x)$, dependent on the position, *x*, of the *dx* element. Following Eq. (12), the Fourier transform of the *dx* segment with the attenuation is

$$G_{dx}'(f)\approx P(f)S(f)h(x)[1+\Phi(f,x)]e^{-2\alpha(f)x}. \tag{30}$$

The average, windowed power spectrum is obtained by integrating the *dx* segments over the gate length, *L*, giving

$$\langle G_{dx}'(f)\rangle\approx\frac{P(f)S(f)}{L}\times\int_0^L h(x)[1+\Phi(f,x)]e^{-2\alpha(f)x}dx. \tag{31}$$

Assuming that the second integral term is negligible then the attenuation function adjusted for the window shape is found by integration of the first term.

A popular window function that is often used is the Hanning window defined as

$$h(x)=\begin{cases}\dfrac{N}{2}\left[1-\cos\left(\dfrac{2\pi x}{L}\right)\right], & 0\leqslant x\leqslant L\\ 0 \quad \text{otherwise}\end{cases}, \tag{32}$$

where *N* is a normalization factor. Insertion of the Hanning window into Eq. (31) and integration of the first integral term yields

$$\int_0^L h(x)e^{-2\alpha(f)x}dx=\frac{N}{2}\left[\frac{1-e^{-2\alpha(f)x}}{2\alpha(f)L\left(1+\left[\dfrac{2\alpha(f)L}{2\pi}\right]^2\right)}\right]. \tag{33}$$

The attenuation-compensation function for the gated signal using a Hanning window follows from Eq. (16) giving

$$A_{\mathrm{OO}_{\mathrm{Han}}}(f,L)=A_{\mathrm{OO}}(f,L)\cdot\left[\frac{2}{N}\left(1+\left[\frac{2\alpha(f)L}{2\pi}\right]^2\right)\right]^2. \tag{34}$$

The normalization factor is found by noting that the attenuation-compensation function reduces to $e^{4\alpha_0(f)x_0}$ as the gate length goes to zero. As $L\rightarrow 0$, $A_{\mathrm{OO}}\rightarrow e^{4\alpha_0(f)x_0}$ and $A_{\mathrm{OO}_{\mathrm{Han}}}$ becomes

$$A_{\mathrm{OO}_{\mathrm{Han}}}(f,L)=\left(\frac{2}{N}\right)^2 e^{4\alpha_0(f)x_0}. \tag{35}$$

Setting Eq. (35) equal to $e^{4\alpha_0(f)x_0}$ gives the normalization factor for the Hanning window

$$N=2.$$

Simulations of scattered signals from Gaussian-type scatterers were also run using the Hanning window. Estimates of scatterer size were made using the Oelze and O'Brien attenuation-compensation function with the Hanning window adjustment and compared with estimates using other attenuation-compensation algorithms.

## III. SIMULATION RESULTS

Numerical simulations were constructed to test the ability of the attenuation-compensation algorithms to account for the frequency-dependent losses and to determine the best algorithm to use. The numerical simulations were made by constructing a random matrix of scattering particles within a length of propagating medium of speed 1540 m/s. A transmitted pulse was constructed as the reference pulse, shown in Fig. 3. The reference pulse had a central frequency of about 8 MHz.

From each point in the matrix where a scattering particle was located, the reference pulse was scattered by multiplying the reference pulse by the form (or shape) factor of the scatterer. The form factor used in the simulations was the Gauss-

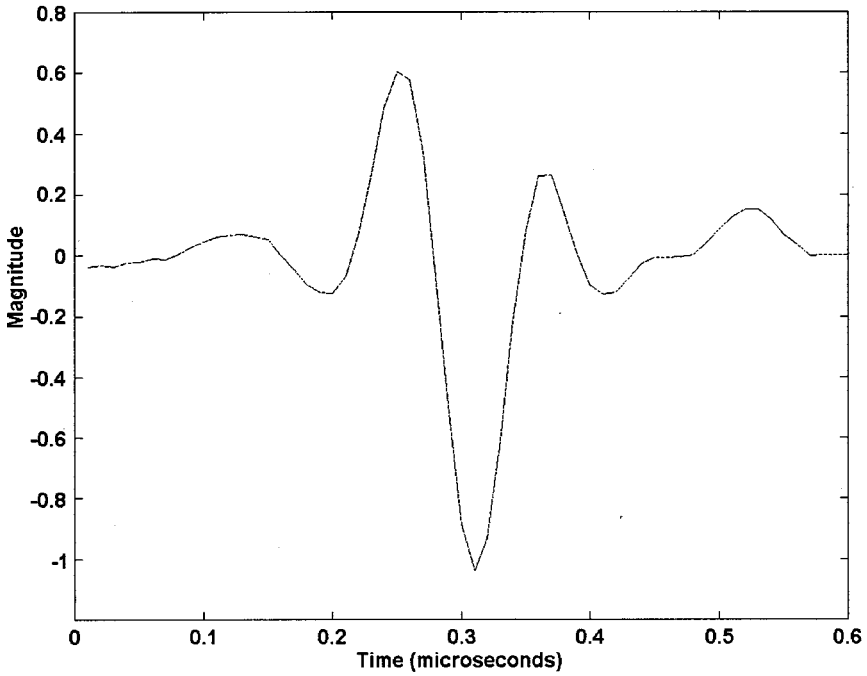


FIG. 3. Reference pulse used in the random scatterer simulations.

ian form factor. The simulated particles scattered according to the Gaussian form factor with an average effective diameter of 49 $\mu$m. An average diameter of 49 $\mu$m and an analysis bandwidth of 4–9 MHz were chosen because they allowed the *ka* value (acoustic wave number times average scatterer radius) to be less than 1.2 over the analysis bandwidth. Insana *et al.*[6,7] showed that by keeping the *ka* value less than 1.2 the most accurate estimations of scatterer diameter could be obtained. The scattered pulses were then combined to create a single backscattered wavetrain. The time location of each scattered pulse depended on the location of the scatterer from the idealized source. In the attenuating medium simulation, the same matrix was used to construct the backscattered wave train except the scattered pulses were also reduced by the frequency-dependent attenuation corresponding to the distance of the scatterer from the source. A total of 25 random matrices were used for both the attenuated simulation and unattenuated simulation in order to obtain an average for the normalized power spectrum. Figure 4 shows a picture of a backscattered signal from an attenuated and an unattenuated simulated medium.

Estimates of average effective scatterer size were obtained by minimizing the average squared difference (MASD) between the normalized power spectrum obtained

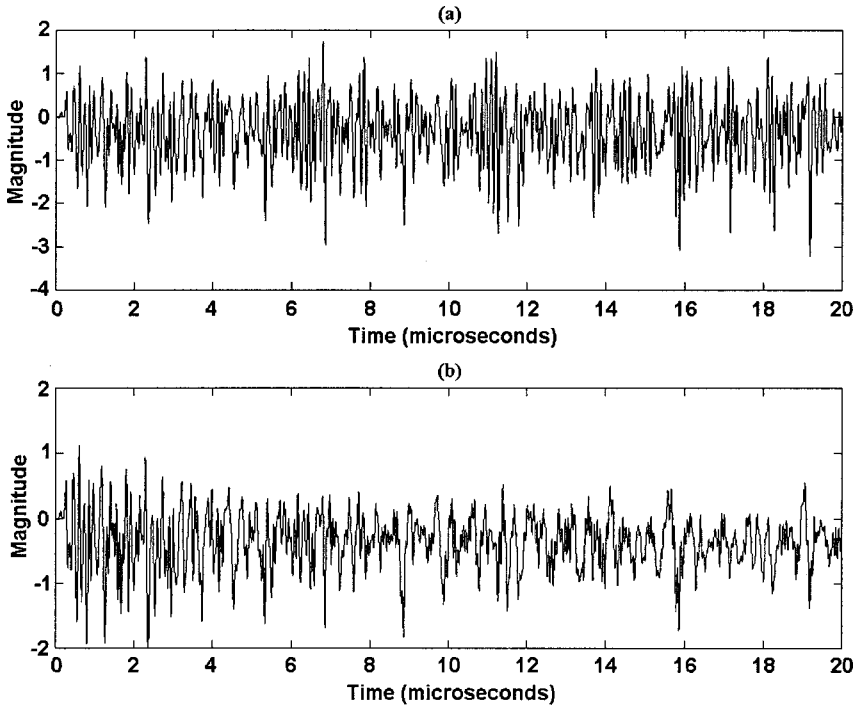


FIG. 4. Backscattered echos from a simulated medium with random scatterers when frequency-dependent attenuation is not present and attenuation is present; (a) unattenuated wave train; (b) attenuated wave train.

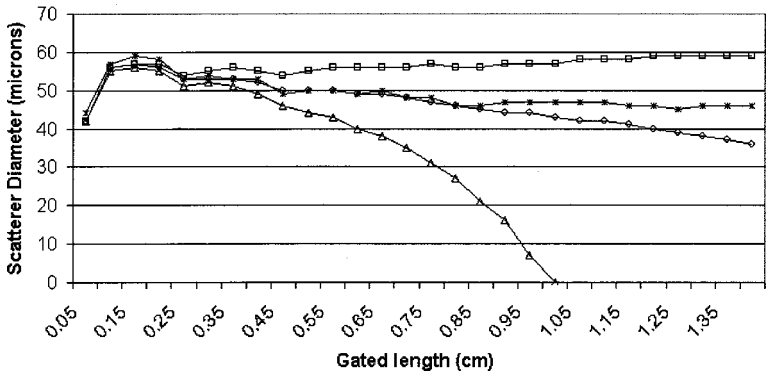


FIG. 5. Scatterer diameter estimations from simulated backscatter returns of randomly distributed Gaussian scatterers with average diameters of 49 micrometers using different attenuation-compensation algorithms and an unattenuated backscatter return, $\alpha = 7 \times 10^{-9} f^{1.19}$ Np/cm; (△) point compensation; (□) O'Donnell and Miller compensation; (◇) Oelze and O'Brien compensation; (*) unattenuated estimates.

from gated segments of the backscattered signal and the Gaussian form factor.[6] The MASD is defined as

$$\mathrm{MASD} = \min\left( \frac{1}{m} \sum_{i=1}^{m} (X_i - \overline{X})^2 \right) \tag{36}$$

with

$$X_i = 10 \log[ W_{\mathrm{meas}}(f_i) / f_i^4 F_{\mathrm{Gauss}}(a_{\mathrm{eff}}, f_i) ] \tag{37}$$

and

$$\overline{X} = \frac{1}{m} \sum_{i=1}^{m} X_i , \tag{38}$$

where $m$ is the number of points in the frequency data bandwidth. The estimate of the average scatterer diameter is the argument that minimizes Eq. (36). The simulations were constructed so that there was no attenuation in the intervening medium ($e^{-2\alpha_0(f)x_0} = 1$). Estimates obtained from the unattenuated signal were used as the standard or control measurement. Estimates were then calculated from the attenuated signal without compensating for attenuation loss and by using the different compensation algorithms. Figure 5 shows the average scatterer diameters estimated from the unattenuated signal and attenuated signals compensated with point attenuation-compensation, the O'Donnell and Miller compensation function, and the Oelze and O'Brien compensation function. The frequency-dependent attenuation used in the simulation is a power law. The Oelze and O'Brien compensation algorithm gives the closest estimate of average scatterer diameter to the estimate by the unattenuated signal. As $\alpha(f)L$ continues to increase, all of the attenuation-compensation functions give estimates of scatterer diameter that diverge from the unattenuated case. The point attenuation and the Oelze and O'Brien attenuation-compensation functions cause an underestimation of the average scatterer diameter while the O'Donnell and Miller attenuation-compensation scheme gives an overestimation of the average scatterer diameter. This means that there exists some optimal attenuation-compensation routine between the Oelze and O'Brien compensation function and the O'Donnell and Miller compensation function.

The percent differences between the scatterer size estimates from the unattenuated signal and the attenuated signal, with and without compensation, are shown in Figs. 6 and 7, respectively. The attenuation used in Fig. 6 is much less than the attenuation used in Fig. 7. The attenuation values were chosen to represent possible values observed for soft tissues.[4,19,20] A comparison between Figs. 6 and 7 shows that with the higher attenuation, the divergence between the control measurement and the compensated measurements occurs at much shorter gate lengths. For example, the percent difference between the unattenuated estimates and the O'Donnell and Miller compensated estimates differ by 10% at a gate length of 7–8 mm for the smaller attenuation (Fig. 6) and at a gate length of about 4.5 mm for the higher attenuation (Fig. 7).

A further examination of Figs. 6 and 7 shows that not compensating for the effects of frequency-dependent attenuation on the power spectrum have immediate consequences on the estimation of average scatterer diameter. Not compensating the normalized power spectrum leads to poor estimates of scatterer sizes. For the lower attenuation case, the point compensation term gives good results for average scatterer size when the gate length is less than 1.25 cm. For the higher attenuation case, the point attenuation gives very poor

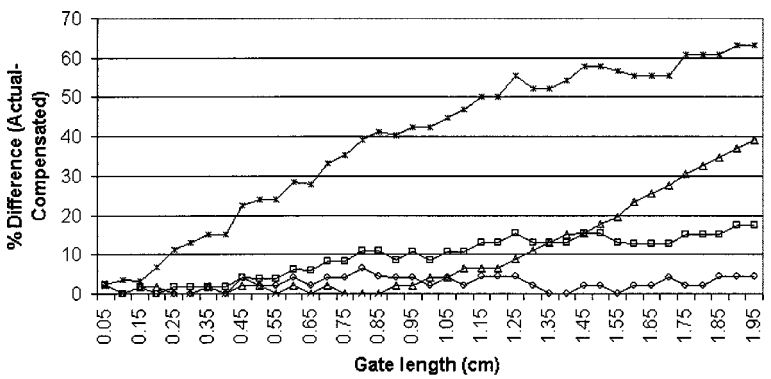


FIG. 6. Comparison of the present difference between the estimation of average scatterer diameter between the unattenuated scatter returns and attenuated scatter returns with various compensation routines, $\alpha = 7 \times 10^{-9} f^{1.13}$ Np/cm; (△) point compensation; (□) O'Donnell and Miller compensation; (◇) Oelze and O'Brien compensation; (*) uncompensated.

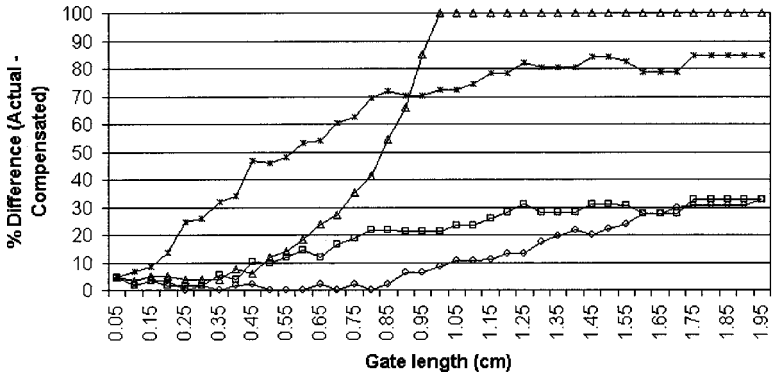


FIG. 7. Comparison of the percent difference between the estimation of average scatterer diameter between the unattenuated scatter returns and attenuated scatter returns with various compensation routines, $\alpha = 7 \times 10^{-9} f^{1.19}$ Np/cm; (△) point compensation; (□) O'Donnell and Miller compensation; (◇) Oelze and O'Brien compensation; (*) uncompensated.

estimates after a gate length of only 4 mm. The estimation by the point attenuation diverges much more rapidly than the other compensation schemes especially for the larger attenuation.

For the lower attenuation case, the Oelze and O'Brien compensation function gives estimates that are smaller than 10% over all gate lengths from the unattenuated estimations while the O'Donnell and Miller scheme gives errors of almost 20% at the larger gate lengths. In the higher attenuation case with a gate length of 8 mm, the Oelze and O'Brien compensation function gives estimates that are more than 20% better than the O'Donnell and Miller compensation function. Increasing the accuracy of estimates of scatterer size by 20% could be significant to applications that utilize this information, i.e., diagnosing tissue disease from average cell size. Comparisons of the O'Donnell and Miller compensation function with the Oelze and O'Brien compensation function show that better estimates can be obtained with the Oelze and O'Brien compensation term when scattering follows the Gaussian form factor.

Simulations were also run in which the time signal was gated using a Hanning window. Estimates were made of the average scatterer diameter from the signal gated with a Hanning window using the Oelze and O'Brien attenuation-compensation function, the O'Donnell and Miller attenuation-compensation function, and the Oelze and O'Brien attenuation-compensation function adjusted for the Hanning window according to Eq. (34). Figure 8 shows the percent difference between the estimates made using the different attenuation-compensation functions. The adjusted Oelze and O'Brien attenuation-compensation function yielded superior estimates of the average scatterer diameter over the other attenuation-compensation functions.

## IV. OPTIMIZATION FOR LARGE ATTENUATION

The expected variance of measurements of particle diameters for particles following the Gaussian form factor has been calculated.[21] The expected variance of the measured average scatterer diameter using the MASD scheme has been shown to be inversely proportional to the actual average scatterer diameter squared.[21] The measurement is less sensitive to smaller average scatterer diameters. In terms of the normalized power spectrum, the fact that the measurement is less sensitive to smaller scatterers means that the normalized power spectrum is changing more slowly with frequency for smaller scatterer sizes, i.e., the overall slope for Gaussian form factor is flatter as seen in Fig. 1. Better estimates are made when the variability of the measured spectrum with frequency is greater rather than smaller.

Undercompensating the attenuation effect by a certain amount will give a more rapidly decreasing overall slope for the normalized power spectrum and a larger estimation of the average scatterer diameter. Overcompensating the attenuation by the same amount will give a smaller estimation of the average diameter. The overcompensation leads to a larger variance in the measurement. What this means for attenuation compensation is that it is better to undercompensate for the attenuation than to overcompensate by the same amount.

Furthermore, attenuation usually increases with increasing frequency. As the attenuation or gate length increases, the signal to noise ratio in the higher frequency components of

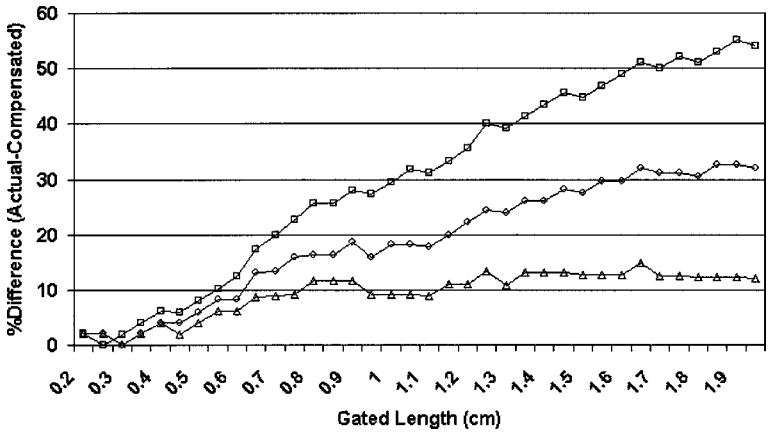


FIG. 8. Comparison of the percent difference between the estimation of average scatterer diameter between the unattenuated scatter returns and attenuated scatter returns using the Hanning window and various compensation routines, $\alpha = 8 \times 10^{-8} f$ Np/cm; (△) Oelze and O'Brien (Hanning adjusted) compensation; (□) O'Donnell and Miller compensation; (◇) Oelze and O'Brien compensation.

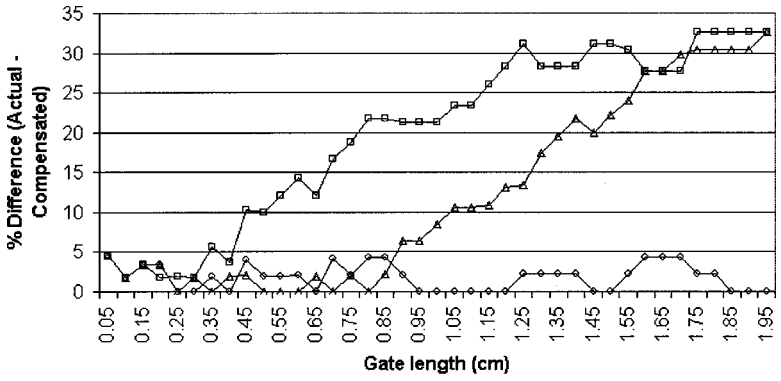


FIG. 9. Comparison of accuracy of different attenuation-compensation techniques vs increasing gate length with $\alpha = 7 \times 10^{-9} f^{1.19}$ Np/cm; (◇) combined compensation; (□) O'Donnell and Miller compensation; (△) Oelze and O'Brien compensation.

the normalized power spectrum becomes smaller. The attenuation-compensation functions compensate the attenuation losses but also amplify the noise. The amplification of noise, especially at high frequencies, tends to make the slope of the normalized power spectrum appear flatter and overcompensation occurs. When the signal to noise is small due to large attenuation, it is better to slightly undercompensate the normalized power spectrum for the attenuation losses. Evidence that undercompensation can yield better results when the signal is noisy can be seen from Figs. 7 and 5. From Fig. 5 it is seen that the O'Donnell and Miller compensation function yielded estimations that were larger in size than the actual (undercompensated) while the Oelze and O'Brien compensation function yielded smaller diameter estimations (overcompensated). Figure 7 shows that the O'Donnell and Miller compensation function, which undercompensates the attenuation losses, begins to give better results as the gate length and frequency-dependent attenuation losses become greater because of the noise effect.

Figure 2 shows the magnitude of the compensation terms versus increasing values of $\alpha(f)L$. From Fig. 2 it is seen that the O'Donnell and Miller compensation function give the smallest attenuation correction to the normalized power spectrum, point compensation gives the largest correction, and Oelze and O'Brien compensation lies somewhere in between. Even though the Oelze and O'Brien compensation function appears to yield a power spectrum that is closer to the unattenuated normalized power spectrum, with large enough $\alpha(f)L$ the O'Donnell and Miller compensation will yield better scatterer size estimations.

The Oelze and O'Brien compensation term leads to an underestimation of the average scatterer size with large $\alpha(f)L$ and the O'Donnell and Miller compensation gives an overestimation of the average scatterer diameter. By combining the two approaches, the estimation of average scatterer sizes can be optimized for large $\alpha(f)L$. At small to medium $\alpha(f)L, \alpha(f)L < 1$, the Oelze and O'Brien compensation function should be used and at larger $\alpha(f)L$ a weighted average of the Oelze and O'Brien compensation function and O'Donnell and Miller compensation function can be used. A closed-form compensation function accomplishing the combined approach can be obtained by use of an interpolation function, $I(\alpha(f)L)$, giving

$$A_{\text{comb}} = A_{\text{OO}} I(\alpha L) + [1 - I(\alpha L)](A_{\text{OO}} + 3A_{\text{OM}})/4, \quad (39)$$

where

$$I(\alpha L) = \frac{2}{1 + \exp(\alpha L/2)}.$$

In this particular case, a three to one weighting in favor of the O'Donnell and Miller attenuation-compensation function was found empirically to give the best estimates of scatterer diameter. As $\alpha(f)L$ becomes large, $\alpha(f)L > 1$, the attenuation compensation switches from Oelze and O'Brien compensation to a combined compensation involving both the Oelze and O'Brien compensation function and the O'Donnell and Miller compensation term. Estimations were then obtained with the combined approach using the same backscattered signals from Fig. 7. Figure 9 shows the percent difference between the compensation routines and the estimations obtained from the unattenuated signal. The combined approach continues to keep the accuracy of the Oelze and O'Brien compensation routine at smaller $\alpha(f)L$ and results in a marked improvement of scatterer estimations at large gate lengths ($\alpha(f)L > 1$). The combined approach gives estimates that are consistently less than 5% different from the estimates obtained form the unattenuated signal over all the gate lengths ($\alpha(f)L$) examined.

## V. CONCLUSIONS

Compensating for the frequency-dependent attenuation loss of a signal in a medium is necessary to accurately estimate scatterer properties such as average scatterer diameter. Several methods exist for compensating the attenuation losses to the normalized power spectrum. The ability of the attenuation-compensation functions to accurately compensate for the attenuation losses depends on the relative size of $\alpha(f)L$. For small $\alpha(f)L, \alpha(f)L < 0.5$, most attenuation-compensation routines yield accurate results. When $\alpha(f)L$ becomes larger, some attenuation-compensation routines overcompensate leading to an underestimation of the scatterer sizes while other compensation routines undercompensate leading to an overestimation of scatterer sizes.

A new attenuation-compensation function was developed. The new attenuation-compensation function was then compared with other compensation functions through numerical simulations of random scattering media. The new attenuation-compensation function was found to give superior results to previous compensation routines except at very

large $\alpha(f)L, \alpha(f)L > 1$. At large $\alpha(f)L$ all attenuation-compensation routines lead to increasingly overestimation or underestimation of scatterer sizes.

When the attenuation is large, it is better to undercompensate the losses to the normalized power spectrum through frequency-dependent attenuation than to correctly compensate the attenuation losses because of the amplification of noise at the high frequencies. Analysis of the attenuation-compensation routines and their ability to properly estimate average scatterer diameter showed that the O'Donnell and Miller compensation function tended to give overestimates of the scatterer sizes. The Oelze and O'Brien attenuation-compensation routine gave an underestimation of scatterer size at large $\alpha(f)L$. The scattering amplitude at the higher frequencies will be smaller for the Gaussian form factor than at the lower frequencies. Attenuation causes the signal to noise ratio to decrease, especially at the higher frequencies. The amplification of noise at the high frequencies leads to an underestimation of the scatterer size from the compensated, normalized power spectrum.

An improvement to the overall attenuation compensation was achieved by combining two compensation functions through an interpolation function. The analysis indicates that the Oelze and O'Brien compensation routine yields a normalized power spectrum that is closest to the unattenuated case. However, because the O'Donnell and Miller compensation function undercompensates, then, as $\alpha(f)L$ becomes large enough, the O'Donnell and Miller compensation begins to give improved estimations over the Oelze and O'Brien compensation function. At lower values of $\alpha(f)L$, less than one, the attenuation compensation followed the Oelze and O'Brien compensation function. At larger values of $\alpha(f)L$, greater than one, the compensation was achieved through a weighted average between the O'Donnell and Miller and the Oelze and O'Brien compensation functions. The combined approach yielded estimates of scatterer size close to the unattenuated case for all values of $\alpha(f)L$ examined using the Gaussian form factor. If other form factors are used to describe scattering from random media, it may be that different combinations of the O'Donnell and Miller and the Oelze and O'Brien compensation functions would yield improved estimates.

The windowing function used to gate the rf time signal must also be accounted for to correctly compensate the attenuation losses to the normalized power spectrum. An adjustment to the Oelze and O'Brien attenuation-compensation function based on the type of windowing function can be easily implemented using Eq. (31). Accounting for the effects of the window on the normalized power spectrum has been shown necessary to accurately estimate scatterer properties.

In choosing an appropriate attenuation-compensation function, several factors need to be considered. The magnitude of the attenuation and the analysis frequency bandwidth must be taken into account. The attenuation may be small at low frequencies and relatively high at large frequencies. According to the simulations, the Oelze and O'Brien attenuation-compensation function will give better estimates for the smaller attenuation. However, if large attenuation of the higher frequencies in the analysis bandwidth leads to small signal to noise, then the Oelze and O'Brien attenuation compensation may not be the best choice for particular frequencies. If there is a small signal to noise ratio at the higher frequencies, then it is better to undercompensate those frequencies. Future work in this area would be to catalog the appropriate attenuation-compensation function or combination of functions for a particular gate length, window type, analysis bandwidth, form factor describing the scattering, frequency dependence, and magnitude of the attenuation.

## ACKNOWLEDGMENT

This work was supported by NIH Grant Nos. CA09067 and CA79179.

[1] F. L. Lizzi, M. Greenbaum, E. J. Feleppa, and M. Elbaum, "Theoretical framework for spectrum analysis in ultrasonic tissue characterization," J. Acoust. Soc. Am. **73**, 1366–1371 (1983).
[2] F. L. Lizzi, M. Ostromogilsky, E. J. Feleppa, M. C. Rorke, and M. M. Yaremko, "Relationship of ultrasonic spectral parameters to features of tissue microstructure," IEEE Trans. Ultrason. Ferroelectr. Freq. Control **34**, 319–329 (1987).
[3] J. A. Campbell and R. C. Waag, "Normalization of ultrasonic scattering measurements to obtain average differential scattering cross sections for tissues," J. Acoust. Soc. Am. **74**, 393–399 (1983).
[4] D. Nicholas, "Evaluation of backscattering coefficients for excised human tissues: Results, interpretation and associated measurements," Ultrasound Med. Biol. **8**, 17–22 (1979).
[5] D. K. Nassiri and C. R. Hill, "The use of angular scattering measurements to estimate structural parameters of human and animal tissues," J. Acoust. Soc. Am. **79**, 2048–2054 (1986).
[6] M. F. Insana, R. F. Wagner, D. G. Brown, and T. J. Hall, "Describing small-scale structure in random media using pulse-echo ultrasound," J. Acoust. Soc. Am. **87**, 179–192 (1990).
[7] M. F. Insana and T. J. Hall, "Parametric ultrasound imaging from backscatter coefficient measurements: Image formation and interpretation," Ultrason. Imaging **12**, 245–267 (1990).
[8] M. F. Insana, "Modeling acoustic backscatter from kidney microstructure using an anisotropic correlation function," J. Acoust. Soc. Am. **97**, 649–655 (1995).
[9] T. J. Hall, M. F. Insana, L. A. Harrison, and G. G. Cox, "Ultrasonic measurement of glomerular diameters in normal adult humans," Ultrasound Med. Biol. **22**, 987–997 (1996).
[10] A. Ishimaru, *Wave Propagation and Scattering in Random Media* (Academic, New York, 1978).
[11] P. M. Morse and K. U. Ingard, *Theoretical Acoustics* (McGraw–Hill, New York, 1968).
[12] F. L. Lizzi, M. Astor, T. Liu, C. Deng, D. J. Coleman, and R. H. Silverman, "Ultrasonic spectrum analysis for tissue assays and therapy evaluation," J. Imaging Syst. Technol. **8**, 3–10 (1997).
[13] V. Roberjot, S. L. Bridal, P. Laugier, and G. Berger, "Absolute backscatter coefficient over a wide range of frequencies in a tissue-mimicking phantom containing two populations of scatterers," IEEE Trans. Ultrason. Ferroelectr. Freq. Control **43**, 970–977 (1996).
[14] R. A. Sigelmann and J. M. Reid, "Analysis and measurement of ultrasound backscattering from an ensemble of scatterers excited by sine-wave bursts," J. Acoust. Soc. Am. **53**, 1351–1355 (1973).
[15] J. F. Chen, J. A. Zagzebski, and E. L. Madsen, "Tests of backscatter coefficient measurement using broadband pulses," IEEE Trans. Ultrason. Ferroelectr. Freq. Control **40**, 603–607 (1993).
[16] M. O'Donnell and J. G. Miller, "Quantitative broadband ultrasonic backscatter: An approach to nondestructive evaluation in acoustically inhomogeneous materials," J. Appl. Phys. **52**, 1056–1065 (1981).
[17] K. A. Wear, R. F. Wagner, M. F. Insana, and T. J. Hall, "Application of autoregressive spectral analysis to cepstral estimation of mean scatterer spacing," IEEE Trans. Ultrason. Ferroelectr. Freq. Control **40**, 50–58 (1993).

[18] A. V. Oppenheim and R. W. Schafer, *Digital Signal Processing* (Prentice–Hall, Englewood Cliffs, NJ, 1975).
[19] D. K. Nassiri, D. Nicholas, and C. A. Miles, ''Attenuation of ultrasound in skeletal muscle,'' Ultrasonics **17**, 230–232 (1979).
[20] K. A. Topp and W. D. O'Brien, Jr., ''Anisotropy of ultrasonic propagation and scattering properties in fresh rat skeletal muscle *in vitro*,'' J. Acoust. Soc. Am. **107**, 1027–1033 (2000).
[21] P. Chaturvedi and M. F. Insana, ''Error bounds on ultrasonic scatterer size estimation,'' J. Acoust. Soc. Am. **100**, 392–399 (1996).